



HAL
open science

Reconfigurable Flow Platform for Automated Reagent Screening and Autonomous Optimization for Bioinspired Lignans Synthesis

Ehu Camille Aka, Eric Wimmer, Elvina Barré, Natarajan Vasudevan, Daniel Cortes-Borda, Tchirioua Ekou, Lynda Ekou, Mireia Rodriguez-Zubiri, Francois-Xavier Felpin

► **To cite this version:**

Ehu Camille Aka, Eric Wimmer, Elvina Barré, Natarajan Vasudevan, Daniel Cortes-Borda, et al.. Reconfigurable Flow Platform for Automated Reagent Screening and Autonomous Optimization for Bioinspired Lignans Synthesis. *Journal of Organic Chemistry*, 2019, 84 (21), pp.14101-14112. 10.1021/acs.joc.9b02263 . hal-02371113

HAL Id: hal-02371113

<https://hal.science/hal-02371113v1>

Submitted on 19 Feb 2021

HAL is a multi-disciplinary open access archive for the deposit and dissemination of scientific research documents, whether they are published or not. The documents may come from teaching and research institutions in France or abroad, or from public or private research centers.

L'archive ouverte pluridisciplinaire **HAL**, est destinée au dépôt et à la diffusion de documents scientifiques de niveau recherche, publiés ou non, émanant des établissements d'enseignement et de recherche français ou étrangers, des laboratoires publics ou privés.

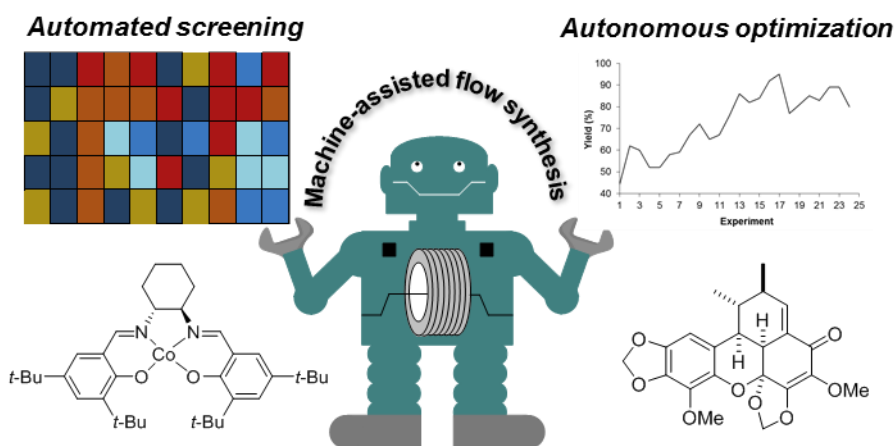
Reconfigurable Flow Platform for Automated Reagent Screening and Autonomous Optimization for Bio-inspired Lignans Synthesis

Ehu Camille Aka,[‡] Eric Wimmer,[‡] Elvina Barré,[‡] Natarajan Vasudevan,[‡] Daniel Cortés-Borda,[‡] Tchirioua Ekou,[†] Lynda Ekou,[†] Mireia Rodriguez-Zubiri,[‡] and François-Xavier Felpin^{*‡}

[‡] Université de Nantes, CEISAM, CNRS UMR 6230, 2 rue de la Houssinière, 44322 Nantes Cedex 3, France

[†] Université Nangui Abrogoua, Laboratoire de Thermodynamique et de Physico-Chimie du Milieu, 02 BP 801 Abidjan 02, Côte d'Ivoire

■ ABSTRACT GRAPHIC



■ ABSTRACT

Naturally occurring benzoxanthenones which belongs to the vast family of lignans, are promising biologically relevant targets. They are biosynthetically produced by the oxidative dimerization of 2-propenyl phenols. In this manuscript, we disclose a powerful automated flow-based strategy for identifying and optimizing a cobalt-catalyzed oxidizing system for the bio-inspired dimerization of 2-propenyl phenols. We designed a reconfigurable flow reactor associating on-line monitoring and process-control instrumentation. Our machine was first configured as an automated screening platform to evaluate a matrix of 4 catalysts (plus the blank) and 5 oxidant (plus the blank) at two different temperatures, resulting in an array of 50 reactions. The automated screening was conducted on micromole scale at a rate of one fully

characterized reaction every 26 minutes. After having identified the most promising cobalt-catalyzed oxidizing system, the automated screening platform was straightforwardly reconfigured to an autonomous self-optimizing flow reactor by implementation of an optimization algorithm in the closed-loop system. The optimization campaign allowed the determination of very effective experimental conditions in a limited number of experiments which allowed to prepare natural products carpanone and polemannone B as well as synthetic analogues.

■ INTRODUCTION

Naturally occurring benzoxanthenones constitute a small group of natural products isolated as racemates and belonging to the vast family of lignans.¹ The most representative members of benzoxanthenone-based natural products include carpanone **1**, polemannone A-C **2-4** and sauchinone **5** and feature a highly oxygenated polycyclic structure with five contiguous stereogenic centers (Figure 1). They have been identified as biologically relevant targets with anti-inflammatory,²⁻³ hepatoprotective,⁴⁻⁵ and antitumor properties.⁶ Synthetic analogues have also been reported to be potent inhibitors of exocytosis and might be useful for the study of vesicular traffic.⁷⁻⁸ Therefore, the significant complexity of the benzoxanthenone skeleton associated to the potential of these structures to interfere with several biological mechanisms, make these structures appealing targets for synthetic chemists.

It has been postulated that the biosynthesis of the benzoxanthenone skeleton occurs through the oxidative dimerization of the corresponding 2-propenyl phenol.¹ This assumption was latter supported by synthetic studies showing that the bio-inspired oxidative dimerization of 2-propenyl phenols using a variety of oxidants such as PdCl₂,⁹⁻¹⁰ [Co]/O₂,¹¹⁻¹² CuCl₂/(-)-sparteine/O₂,¹³⁻¹⁴ PhI(OAc)₂⁷⁻⁸ and laccase,¹⁵ indeed furnishes the benzoxanthenone skeleton. We recently described the multi-step synthesis of carpanone **1** in flow using a modular autonomous flow reactor.¹⁶ Advantages of conducting reactions in flow with respect to traditional batch reactors include higher mass and heat transfers, better reproducibility, improved kinetics, safer experimental conditions and easier automation.¹⁷⁻²⁴

In our approach, all discrete steps of the flow synthetic route were optimized with the use of a black-box optimization algorithm working without *a priori* reaction and gradient information. In particular, the oxidative dimerization furnishing carpanone **1** was optimized in

1,2-dichloroethane using molecular oxygen as the oxidant associated to a $\text{Co}^{\text{II}}(\text{salen})$ complex as the catalyst.

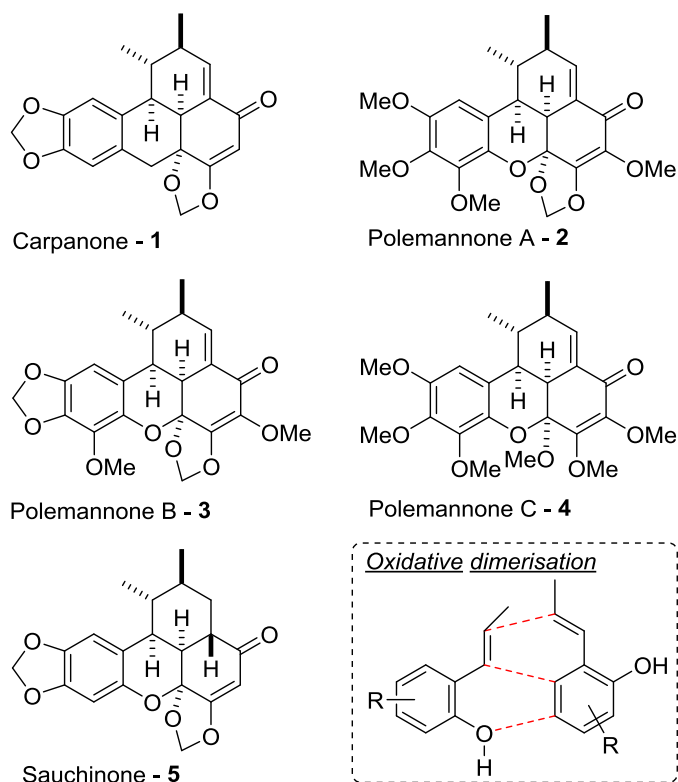


FIGURE 1. Naturally occurring benzoxanthenones lignans. Oxidative dimerization of 2-propenyl phenols as inset.

While these experimental conditions furnished carpanone **1** in 82% isolated yield, we later faced difficulties to prepare multi-gram amounts of carpanone **1** for two reasons. First, under the optimal conditions, carpanone **1** was prepared with an excellent isolated yield (82%) but with a modest productivity (ca. 17 mg/h) due to the high dilute experimental conditions (ca. 0.015 M) and the modest kinetic (ca. 40 min residence time). Second, the use of a stock solution of 1,2-dichloroethane saturated with pure oxygen posed severe safety concerns for our industrial partner in charge of the scaling-up.²⁵ While the first issue could be addressed with an increase of the initial concentration of starting materials, the second issue required us to reinvestigate the oxidative conditions through the screening of alternative oxidants and catalysts compatible with a flow regime. The experimental flow setup we developed for the synthesis of carpanone in our previous investigations was not adapted for reagents screening as it would require the use of three streams for the starting material, oxidant and catalyst, respectively. This also implies that an automated screening of oxidants and catalysts was not possible as it would require a manual change of the stock solutions. In this manuscript, we

report the development of a reconfigurable and intelligent synthesis platform that allows both automated micromole-scale reagent screening and autonomous reaction optimization in flow. The automated platform includes a number of benefits as it allows very reproducible experiments on a micromole scale due to the use of a liquid handling robot and minimizes the consumption of solvent due to the use of a single stream. Additionally, the use of a liquid handling robot in charge of the reaction mixture preparation prevents issues associated with the reproducibility of the mixing process.

This machine led to the discovery of uncovered oxidative conditions for the construction of the benzoxanthenone skeleton and allowed the synthesis of naturally occurring capanone **1** and polemannone B **3** as well as a synthetic analogue.

■ RESULTS AND DISCUSSION

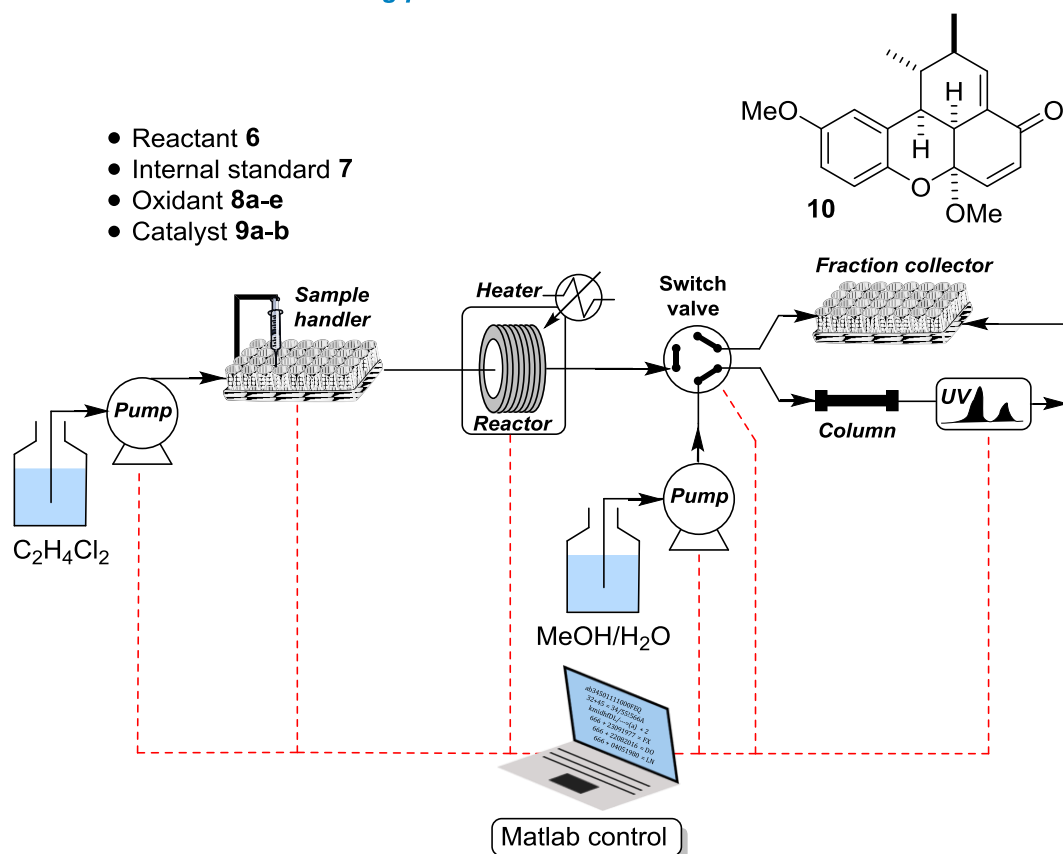
The bio-inspired oxidative dimerization of 2-propenyl phenols has been reported in batch under a variety of experimental conditions which are, for most of them, unsuitable for flow conditions due to either solubility issues (PdCl₂, laccase) or long reaction times (CuCl₂/(-)-sparteine/O₂, 24 h). We demonstrated that the use of Co^{II}(salen)/O₂ as the oxidizing system could be efficiently transferred from batch to continuous flow conditions;¹⁶ however, the use of molecular oxygen was associated with safety concerns, especially in the industrial environment. Considering that the reasonable price of cobalt-based catalysts was an important asset, we decided to explore the combination of a selection of commercially available Co catalysts with oxidants compatible with flow conditions to properly address safety concerns for scaling-up experiments; keeping in mind that oxidants are, by nature, hazardous compounds requiring careful handling, especially on large scale.

In our initial experimental procedure, a stock solution of cobalt catalyst in 1,2-dichloroethane was saturated with oxygen gas (O₂).¹⁶ While this protocol features an obvious simplicity reaching the main principles of sustainable chemistry,²⁶ it suffers from safety concerns upon scaling-up, as the stock solution could represent a highly flammable volume of several liters.²⁷ The other issue associated with this protocol is related to the difficulty in measuring the exact volume of O₂ dissolved in 1,2-dichloroethane so that the amount of oxygen available for the oxidative dimerization could not be precisely determined. This point is particularly relevant upon increasing the concentration of starting material as the amount of oxygen required by unit of

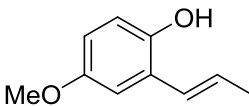
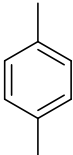
volume would substantially increase until reaching a value where oxygen becomes the limiting reagent. The use of a diluted gas mixture (5-10% O₂ in N₂) is an alternative strategy which allows users to keep the O₂ concentration in the organic solvent below the explosive limit. However, the low amount of O₂ which can be solubilized with such a strategy could preclude the reaction to reach complete conversion.²⁸

With the aim of addressing these limitations we embarked on the search for a new oxidizing system avoiding the use of O₂. In this frame, we designed a new reconfigurable and fully automated screening platform capable of preparing reaction mixture from specified reagents on the μmol scale (Figure 2, see also Figure S2 in SI for a photograph of the platform). Our one-stream system includes a liquid handling robot in charge of the reaction mixture preparation, a pump, a thermostated reactor coil and a switch valve which samples a small fraction of the crude mixture for the on-line HPLC analysis.

Automated screening platform



Reagents screened

Reactant	Internal standard	Oxidant	Catalyst
6 , [0.2 M]	7 , [0.5 M]	[0.4 M]	$[2.5 \times 10^{-3} \text{ M}]$
		8a - <i>t</i> -BuOOH, 8b - Cumene-OOH 8c - PhI(OAc) ₂ 8d - Oxygen 8e - Air	[Co]-9a [Co]-9b [Co]-9c [Co]-9d
Reaction mixture : [0.021 M]			

Catalysts structure

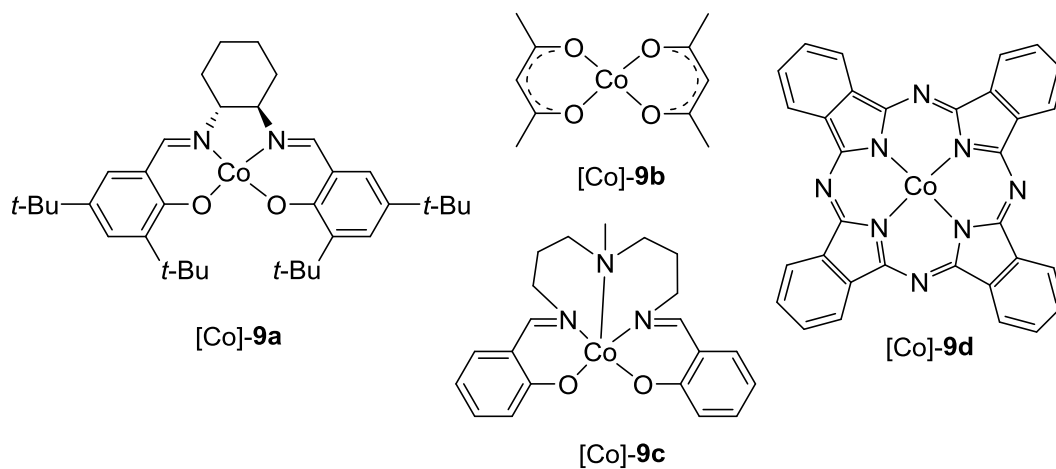


FIGURE 2. Evaluation of oxidizing systems through a μmol scale automated screening platform

An automatic data processing integrates the chromatogram and calculates the yield using an internal standard. All modules from the screening platform are connected to a computer through RS-232 ports and controlled with an ad-hoc process-control software.

To start a screening campaign, an operator populates the 56-well plate with vials containing the required reagents (starting material, catalyst, base...). After having fed the process-control software with the concentration of the stock solution-containing vials, the composition of the reaction mixture, the stoichiometry chosen for the screening and the volume injected in the coil reactor, the sampling robot automatically determines the volume of suction in each vial to prepare the reacting mixture injected in the coil reactor. Two different setups were designed depending on the nature of the oxidant. Non-gaseous oxidants were sampled by the liquid handling robot from the stock solutions and the reaction occurred in a PEEK reactor. Gaseous oxidants such as air and oxygen were supplied to the reaction mixture through the use of a gas-permeable coil reactor made from the AF-2400 polymer.²⁹⁻³⁰ The search for a new oxidizing system using the screening platform was carried out with the benchmark oxidative dimerization of 2-propenyl phenol **6** to benzoxanthone **10**. We prepared a 40-member 3-dimensional array from a selection of 3 non-gaseous oxidants **8a-c** (plus one blank) and 4 cobalt catalysts **9a-d** (plus one blank). The array was split in two runs of 20 experiments carried out at 25 and 50 °C. An additional 10-member 2D array from a selection of catalysts **9a-d** (plus one blank) and 2 gaseous oxidants **8d-e** were conducted at 25 °C. For safety reasons we did not studied gaseous oxidant, and especially oxygen, at 50 °C. In this screening campaign the use of oxygen served as a standard to assess the efficiency of other oxidants screened. To our knowledge, the cobalt-catalyzed oxidative dimerization of 2-propenyl phenols had only been investigated with oxygen as oxidant and the potential of alternative oxidants in promoting the expected dimerization remained to be demonstrated.

Reactions explored with the screening platform were arbitrarily conducted using 4 μmol of **6** with 1.5 equivalents of non-gaseous oxidant and 10 mol% of cobalt catalyst at either 25 or 50 °C. By using a high loading of cobalt catalysts and an excess of oxidant, we minimize the risk of missing an effective Co/oxidant combination. 2-Propenyl phenol **6**, non-gaseous oxidants and cobalt catalysts were prepared as stock solutions in 1,2-dichloroethane at 0.2, 0.4, and 0.0025 M, respectively and placed in the 56-well plate of the liquid handling robot. For the use of gaseous oxidants, the experimental setup was slightly modified by switching the PEEK reactor for a gas permeable tubing reactor made from AF-2400 polymer that passed through a chamber

supplied with a flow of either air or oxygen.²⁹ This procedure differs from the one we previously published and addresses the risk of lacking oxidant when using concentrated solution of 2-propenyl phenols. In order to allow the screening at an elevated throughput, all reactions were conducted at a single residence time of 10 minutes. Each fully automated experiment, including the robot-mediated reaction mixture preparation, the reaction time, the on-line HPLC analysis and the data processing (integration and yield calculation) was completed in *ca.* 26 minutes and the screening campaign was achieved at a rate of 27 experiments every 12 hours; for safety reason the machine was not used overnight. Both oxidants and catalysts were selected for their (i) potential to promote the oxidative dimerization, (ii) solubility in 1,2-dichloroethane, (iii) ease of handling under standard conditions and (iv) commercial availability. Several oxidants were discarded as they were either insoluble in DCE (DDQ and TEMPO) or required aqueous biphasic conditions (H₂O₂ and Oxone[®]).

The analysis of the 50-reaction screen revealed several interesting features (Figure 3). First, reaction conducted at 50 °C consistently gave lower HPLC yields of the targeted benzoxanthene **10**, suggesting a pronounced thermal sensitivity of either starting materials or benzoxanthene **10**. Second, [Co]-**9a-b** gave significantly higher yields than [Co]-**9c-d** whatever the oxidant used. Regarding the effect of oxidants it was observed that all 3 non-gaseous oxidants **8a-c** performed similarly while air and oxygen gave lower yields under such short residence time. These results validated our strategy to switch oxygen for a non-gaseous oxidant. A closer look on background reactions, revealed that PhI(OAc)₄ **8c** was the only oxidant promoting the dimerization in a significant extent in the absence of cobalt catalyst. While the ability of PhI(OAc)₄ **8c** to promote the dimerization of 2-propenyl phenols to benzoxanthene skeletons was already known,⁷⁻⁸ our results show an uncovered exalted reactivity in the presence of cobalt catalysts. Despite the slightly better results obtained with PhI(OAc)₄ **8c**, we selected *t*-BuOOH **8a** as it is less expensive and only produces *t*-BuOH as by-product. Regarding the catalyst selection, both [Co]-**9a** and [Co]-**9b** gave promising results. Despite its much lower price, [Co]-**9b** proved to be particularly insoluble above 2.5×10^{-3} M, precluding any scale-up experiments under more concentrated conditions. We therefore preferred the use of [Co]-**9a** for our further studies. The process for discovering a new cobalt-catalyzed oxidative system for the dimerization of 2-propenyl phenols to benzoxanthene skeletons required 50 reactions at a throughput of one reaction every 26 minutes. Each reaction used 4 μmol of starting material **6** and 0.4 μmol of cobalt catalysts **9a-d**.

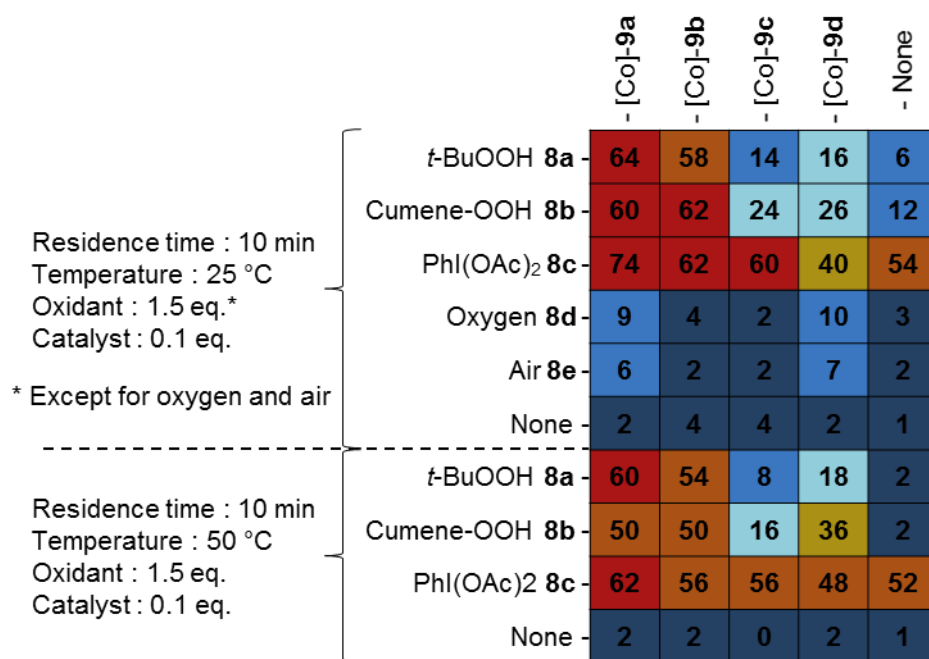


FIGURE 3. Heatmap visualization of the automated micromole-scale screen across a 50-member array.

Having identified [Co]-**9a**/*t*-BuOOH **8a** as the most promising oxidative system from the screening of 50 reactions, we further optimized experimental conditions using an autonomous self-optimizing flow reactor. This emerging technology combines the power of automated flow devices with an assistive optimization algorithm and integrates a quasi-real time in-line/online monitoring.³¹⁻³⁵

In most chemical laboratories, optimizations are traditionally conducted by modifying one factor at a time until reaching an optimum. While the simplicity of execution is the major asset explaining the popularity of this approach, the data obtained fail to explain interactions between variables, precluding any efficient automation. The automated screening of a set of predetermined experimental conditions generated from design-of-experiment (DoE) methods partially addresses the issues of one-factor-at-a-time optimizations. However, multi-variable optimizations using DoE methods usually require a high number of experiments to locate a satisfactory optimum.

The use of feedback algorithms working in black box-type systems is a powerful alternative to traditional one-factor-at-a-time and DoE methods for optimizing chemical reactions.³⁶⁻³⁷ Several black box algorithms of different numerical complexity have been reported in the literature for integration in self-optimizing flow devices.³⁸⁻⁴⁹ From these algorithms, the Nelder-Mead method,⁵⁰ also known as the simplex method, has been reported to be one of the simplest for implementation in automated flow

reactors.⁵¹⁻⁶⁰ Numerically, it is one of the simplest optimization algorithms and does not require gradient approximation which is a strong asset when working with expensive experiments. However, the Nelder-Mead method suffers from two important drawbacks: (i) it does not converge rapidly when optimizing large multi-variable problems and (ii) it only converges to a local optimum which quality highly depends on the initialization and the studied system.⁶¹ We addressed these issues through the development of a profoundly modified version of the Nelder-Mead method that includes (i) the possibility to temporarily modify the dimensionality of the search to explore a subspace, (ii) multiple stopping criteria to lower the number of experiments, (iii) diversification and intensification mechanisms to escape from an unsatisfactory local optimum, (iv) the golden search method for 1-D optimizations which cannot be addressed by the Nelder-Mead method.⁶² Moreover, in addition to the traditional linear constraints imposed by boundary constraints, our algorithm contains an optional mechanism to restrict the search space through linear constraints in order to exclude experimental conditions considered as unsound (lack of reactivity, poor stability of reagents/products...).

The transformation of our automated screening platform to an autonomous self-optimizing flow reactor was straightforward and convenient as the only modification consisted of the integration of our additional optimization algorithm to the process-control software. Our approach allows to either screen discrete variables for reaction development or continuous variables for a fine-tuning of experimental conditions (self-optimization). While the use of automated screening platforms have been described in the literature,⁶³⁻⁶⁸ the use of a reconfigurable platform for either screening or self-optimization offers a much higher flexibility. The optimization was conducted at higher concentrations with stock solutions of 2-propenyl phenol **6**, [Co]-**9a** and *t*-BuOOH **8a** at concentration of 1 M, 0.03 M and 2 M, respectively, in order to assure an elevated throughput.

The reaction yield was optimized in a 4-dimension space where the residence time, temperature, equivalent of *t*-BuOOH **8a** and loading of [Co]-**9a** were selected as input variables in the range of 5-60 minutes, 25-50 °C, 1-2 equivalents, 1-10 mol%, respectively. In addition to the bounded search space, we also fixed the initial point X_0 at 5 minutes of residence time, 25 °C, 1 equivalent of *t*-BuOOH **8a** and 5 mol% of [Co]-**9a** with *d* values of 10 min, 5 °C, 0.2 equivalent and 2 mol%, respectively. While we preferred to focus on the reaction yield optimization, we were also interested in developing experimental conditions

allowing decent productivity. Therefore, for experimental conditions displaying the highest yields, the associated productivity have been considered as well.

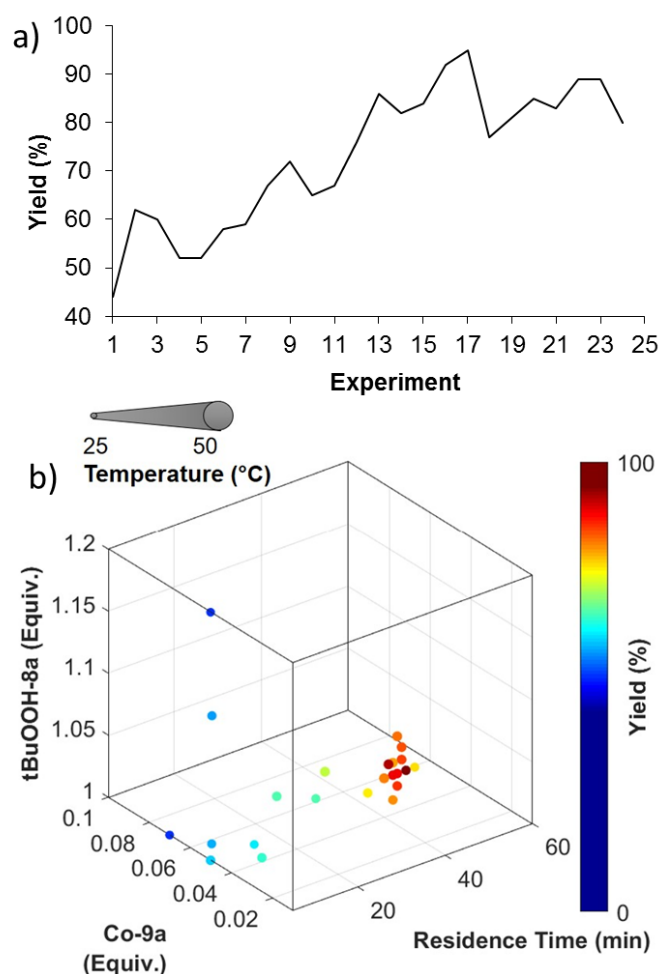
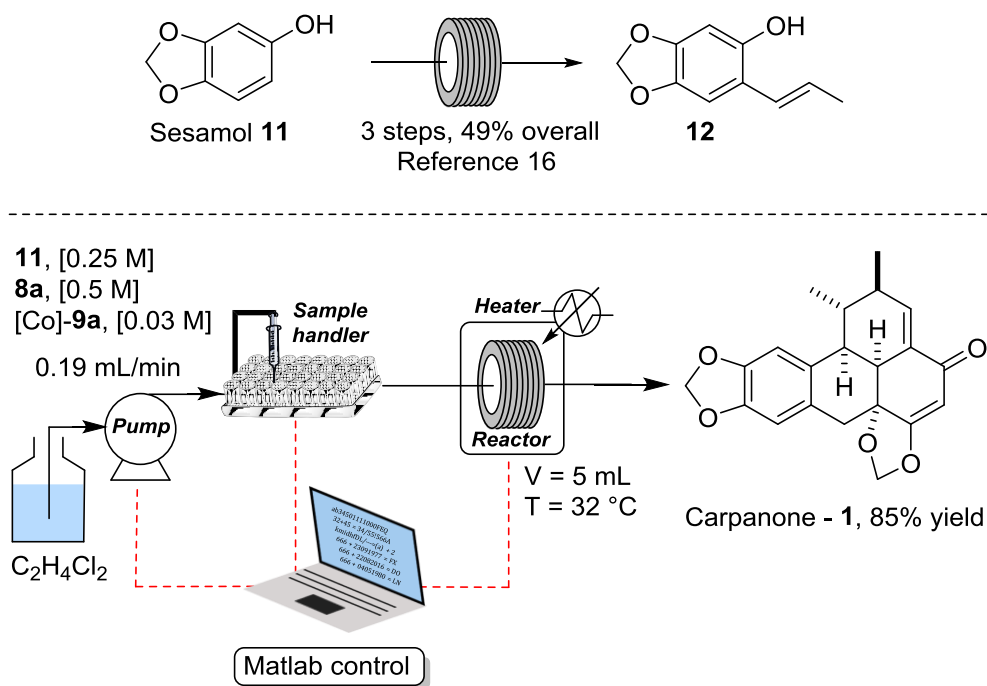


FIGURE 4. (a) Maximization of the yield of benzoxanthenone **10**. (b) Representation of the four-dimensional experimental conditions for the maximization of the yield for benzoxanthenone **10**.

The first 5 experiments corresponding to the initial 4-D simplex, gave promising yields ranging from 44 to 62% (Figure 4a-b, See Table S1 in SI for details). In the subsequent experiments, the algorithm rapidly decreased the loading of [Co]-**9a** until reaching the lower bound at 1 mol%, while in the same time the residence time progressively increased to *ca.* 30 minutes. On the other hand, both the equivalents of *t*-BuOOH **8a** and the temperature were set to *ca.* 1.00-1.10 equivalents and 27-33 °C, respectively. The algorithm reduced the dimension of the search from experiment 17 by fixing the catalyst loading to its lower bound, reaching an optimum corresponding to 95% yield. After 5 consecutive simplexes which did not improve the reaction yield, the algorithm reached a stopping criterion and the optimization

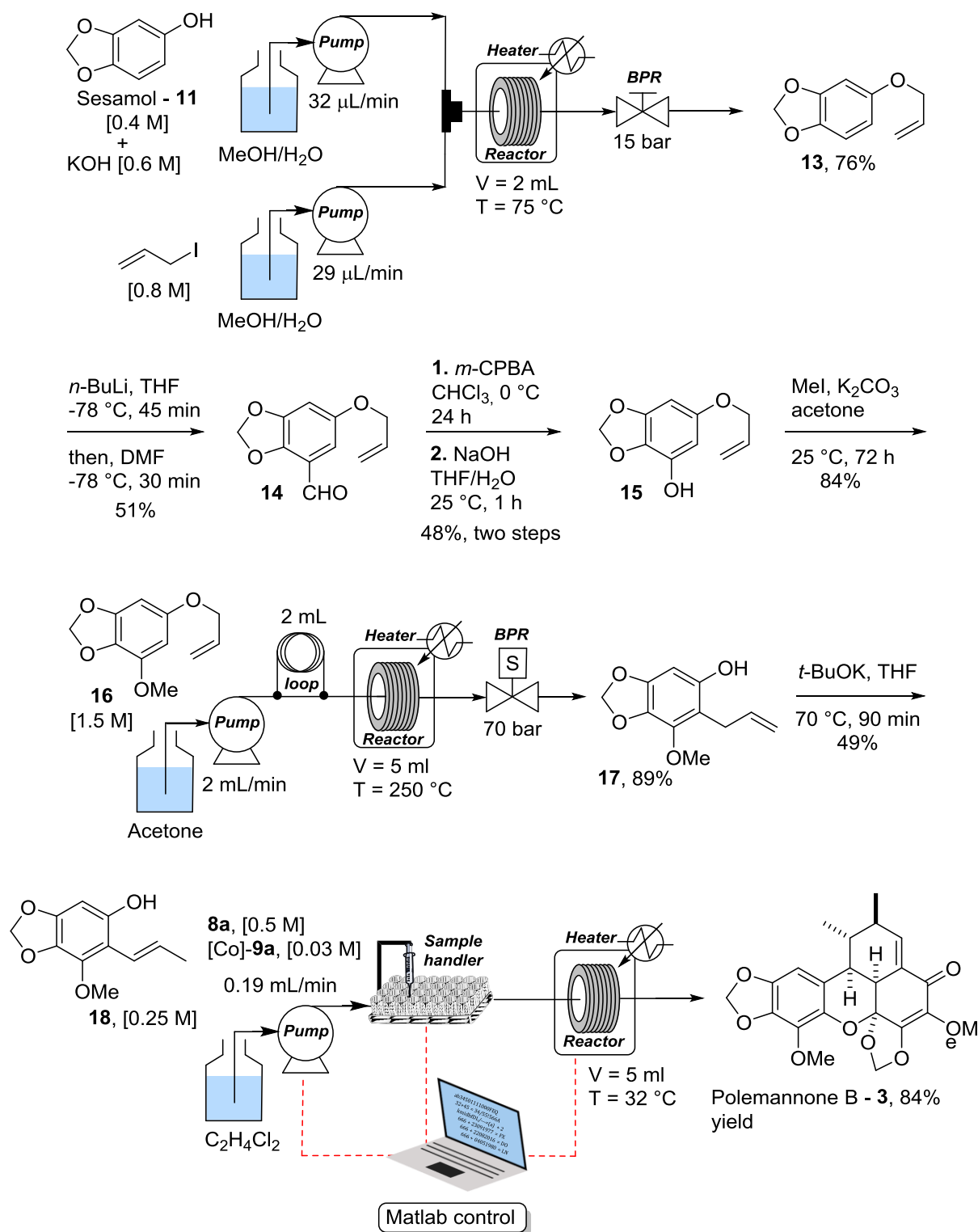
stopped after experiment 24. From the 24 experiments conducted through this optimization campaign, we observed two appealing solutions corresponding to experiments 16 and 17 which led to benzoxanthenone **10** as a single diastereoisomer with 92 and 95% yield, respectively. A closer look on the experimental conditions revealed that experiment 16 (27 minutes, 32 °C, 1.09 equiv **8a** and 1 mol% **9a**) provided a better productivity than experiment 17 (31 minutes, 29 °C, 1.08 equiv **8a**, and 1 mol% **9a**) with values of 887 and 800 mg.h⁻¹, respectively. The calculated productivity for each experiment can be found in Table S1. Unfortunately, upon purification by flash chromatography, benzoxanthenone **10** turned to be extremely instable in our hand, leading to a modest isolated yield (55%).

We further pursued our efforts toward the synthesis of natural lignans carpanone **1** and polemannone B **3** using the optimized conditions from experiment 16. Desmethoxycarpacine **12**, obtained in three steps from sesamol **11** following our previously published flow procedure, was dimerized to carpanone **1** in 85% isolated yield (Scheme 1).¹⁶ A minor isomer, identified on the crude mixture (*ca.* 3%), was lost during the purification step and carpanone **1** was isolated as a single isomer. In such experimental conditions the productivity spectacularly increased from *ca.* 17 mg/h using our previous setup to *ca.* 263 mg/h in this work. The reproducibility of our automated screening platform machine was also assessed with the oxidative dimerization of desmethoxycarpacine **12** to carpanone **1** on 6 consecutive runs in the optimal conditions of experiment 16. The reaction yields calculated by the online HPLC system were 85, 86, 86, 86, 86 and 87%, respectively, corresponding to an average HPLC yield of 86% (*vs* 85% for the isolated yield) and a standard deviation of only 0.63.



SCHEME 1. Improved flow synthesis of carpanone **1** in flow.

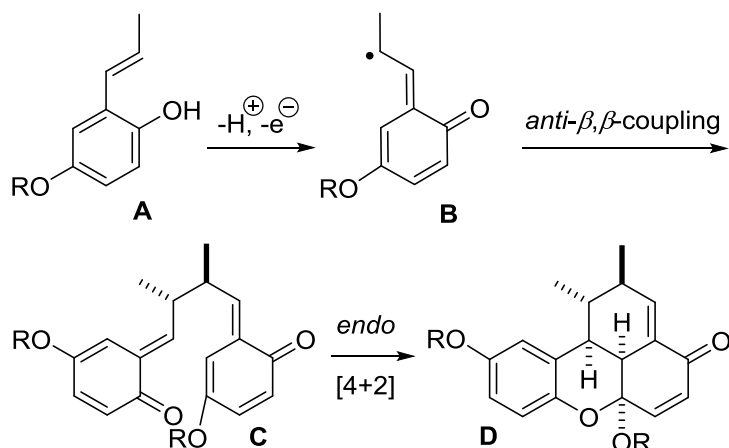
Regarding the total synthesis of polemannonone B **3**, we prepared the required 2-propenyl phenol **17** in 7 steps from commercially available sesamol (Scheme 2). A mixed batch-flow synthesis was developed for the synthesis of **17**. The allylation of sesamol **11** with allyl iodide was conducted in flow providing the corresponding allyl ether **13** in 76% yield. The required methoxy group was installed through a 4-step batch sequence. The formylation of **13** with DMF/*n*-BuLi furnished the expected aldehyde **14** with a modest yield (51%). A Baeyer-Villiger oxidation of aldehyde **14** furnished the formate intermediate which was immediately hydrolyzed with aqueous NaOH to reveal the phenol function of **15** (48%, two steps). The latter was etherified with methyl iodide to give **16** in 84% yield. The thermal [3-3]-Claisen rearrangement was conducted under flow-mode as it provided an improved reaction rate and much safer experimental conditions. The rearrangement occurred in acetone at 250 °C and 70 bar with a residence time of only 2.5 minutes to provide phenol **17** in 89% yield. Under such high-temperature/high-pressure conditions acetone reached its supercritical state.⁶⁹⁻⁷¹ Lastly, allylphenol **17** was isomerized to the corresponding 2-propenyl phenol **18** by treatment with *t*-BuOK in 49% yield. The 8-step total synthesis of polemannonone B **3** was smoothly achieved through the oxidative dimerization of 2-propenyl phenol **18** using the automated platform under optimal conditions developed for the synthesis of **10**, providing polemannonone B **3** in 84% isolated yield as a single isomer. This synthesis complements the still scarce examples of total synthesis of natural products using a mixed batch/flow approach.⁷²



SCHEME 2. Total synthesis of Polemannone B **3** under mixed batch/flow modes.

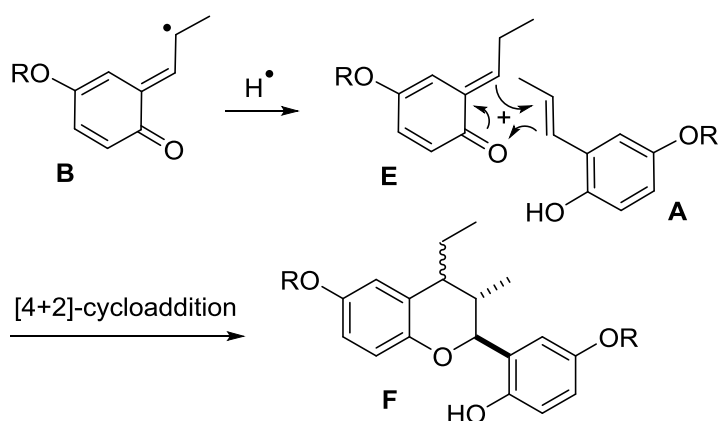
The mechanism of the oxidative dimerization is still a subject of debate which has not led to a unanimous consensus at present; some authors also propose the possibility of several mechanisms depending on the experimental conditions.¹⁰ Though, the most

common mechanism proposed in the literature involves an initial *anti*- β,β -radical dimerization followed by an *endo*-[4+2] cycloaddition (Scheme 3).



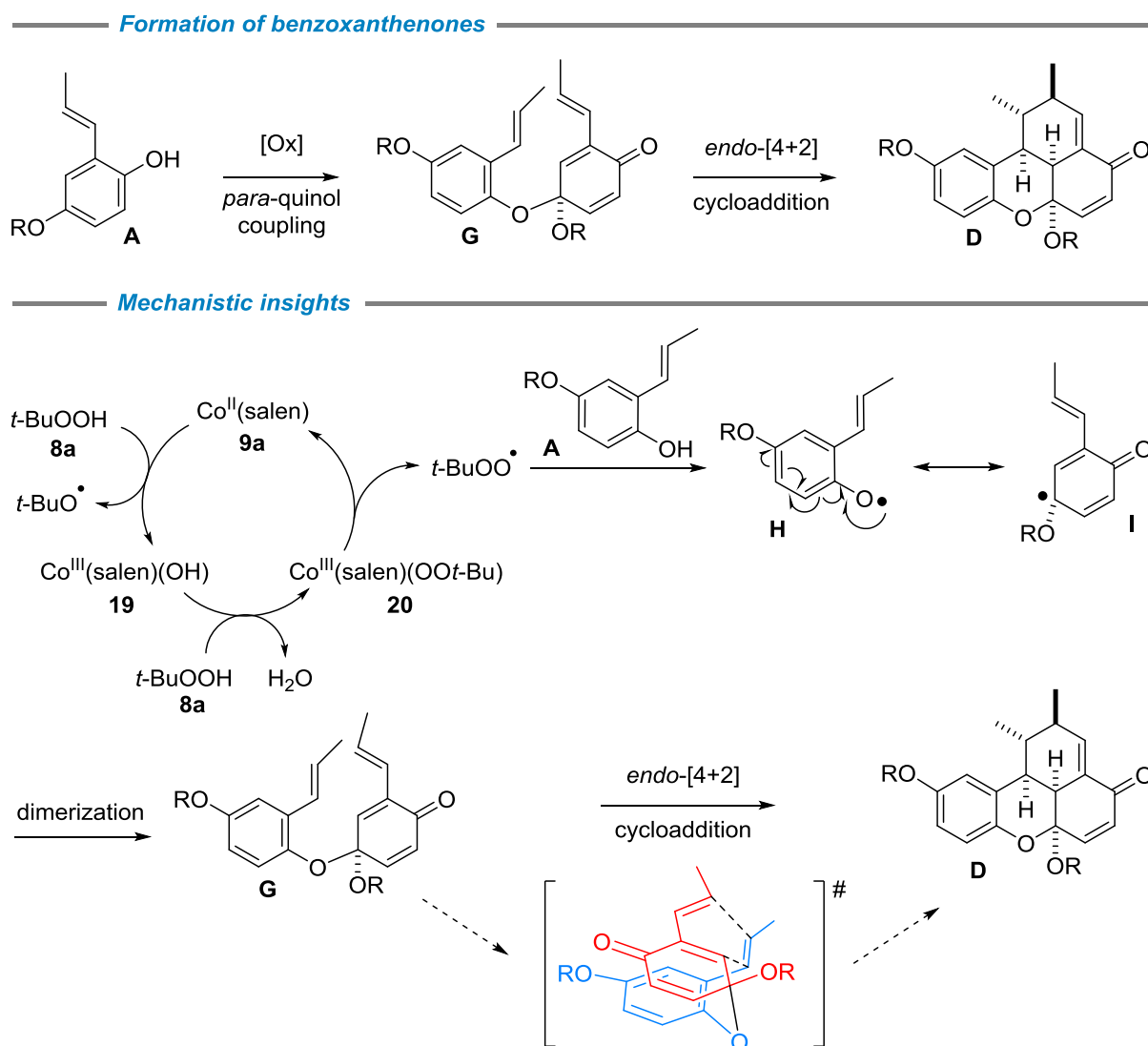
SCHEME 3. Mechanistic proposal involving sequential *anti*- β,β -radical dimerization/*endo*-[4+2] cycloaddition.

However, this mechanistic proposal fails to properly explain the perfect *anti*-selectivity observed at the methyl groups from the β,β -radical dimerization. Moreover, radical **B** would be reactive and could abstract, at least partially, a hydrogen atom from the solvent or the starting phenol, leading to the *ortho*-quinone methide **E** which is known to rapidly dimerize into the corresponding benzopyrane **F** (Scheme 4).¹⁵



SCHEME 4. Dimerization of *ortho*-quinone methides **E** to benzopyrane **F**.

In all our tests, regardless of the oxidant used, we never observed the formation of benzopyrane-type structures. In a previous report we proposed an initial *para*-quinol-type coupling followed by an endo-[4+2] cycloaddition (Scheme 5, top).¹⁶ While this mechanism properly explains the *anti*-selectivity at the methyl group, we did not have any experimental evidence at that time to support this proposal. We have reinvestigated this mechanism, and we are now able to confirm our proposal when using [Co]-**9a**/*t*-BuOOH **8a** as oxidizing system. The oxidation of [Co]-**9a** by *t*-BuOOH **8a** produces the corresponding Co^{III}(salen)(OH) complex **19** along with the *tert*-butoxy radical (Scheme 5, bottom).⁷³ Ligand exchange on Co^{III}(salen)(OH) complex **19** furnishes Co^{III}(salen)(OO*t*-Bu) complex **20** which restored starting cobalt complex **9a** along with *t*-BuOO[•]. The latter abstracts the phenolic hydrogen from **A** to give the corresponding phenoxy radical **H** which by delocalization of the unpaired electron furnishes aryl radical **I**. Dimerization of **H** with **I** furnishes the *para*-quinol-type intermediate **G** which further cyclizes through an endo-[4+2] cycloaddition to give the benzoxanthenone skeleton **D**.



SCHEME 5. Mechanistic proposal for the bio-inspired formation of benzoxanthenones lignans through Co(II)/*t*-BuOOH oxidative dimerization of 2-propenyl phenols.

■ CONCLUSION

In this work we designed a reconfigurable flow reactor which could be used either as an automated screening platform or as an autonomous self-optimizing reactor for natural product synthesis. The capability of our automated screening platform to screen discrete variables on the micromole scale and analyze the crude content through an online monitoring in a short time frame is a strong asset in reaction discovery. By associating process control instrumentation and online analysis to an optimization algorithm in a closed-loop system, the screening platform can be easily transformed to a powerful autonomous self-optimizing flow reactor for the optimization of continuous variables. The automated screening platform identified a new cobalt-catalyzed

oxidative system for the dimerization of 2-propenyl phenols to benzoxanthone skeletons from an array of 50 reactions which represent a total of only 200 μmol (0.66 mg per reaction) of starting material. The cobalt-catalyzed oxidative system identified with the screening platform was further optimized in a 4-dimension space using an autonomous closed-loop system. A very satisfactory optimum was located after only 16 experiments and the system reached a stopping criterion after only 24 experiments. This cobalt-catalyzed oxidizing proved to be particularly efficient to prepare natural products carpanone and polemannon B as well as a synthetic analogue.

Through this work, we demonstrated that while essentially used for preparative procedures, flow reactors are also particularly well suited for automated reagent screening and autonomous reaction optimization. While the development of automation in chemistry is a modern preoccupation,⁷⁴⁻⁷⁹ the results described in this work shows that process control instrumentation associated to menial and assistive algorithms assist chemists and improve their intellectual productivity.

■ EXPERIMENTAL SECTION

General information. All commercially available chemicals were used as received unless otherwise noted. ^1H and ^{13}C NMR spectra were recorded at 300 or 400 and 75 MHz or 100 MHz, respectively. ^1H and ^{13}C NMR spectra were referenced to the internal deuterated solvent (CDCl_3) at 7.26 and 77.16 ppm, respectively. FT-IR spectra were recorded in the ATR mode. Wavelengths of maximum absorbance (ν_{max}) are quoted in wave numbers (cm^{-1}). High resolution mass spectrometry (HRMS) was recorded on a microTOF spectrometer equipped with orthogonal electrospray interface (ESI). Analytical thin-layer chromatography (TLC) was carried out on silica gel 60 F_{254} plates and visualized with a UV lamp at 254 nm or stained with a basic potassium permanganate solution. Flash column chromatography was performed using silica gel 60 (40–63 μm).

Details of the experimental setup. HPLC pumps (JASCO PU2080) equipped with a RS-232 port were employed to flow the solution through the system. A sampler handler (JASCO AS 2055) equipped with a RS-232 port was used to inject the reagents in the line. The reactor coil was heated with a heating plate (Heidolph, MR Hei-Connect) equipped with a RS-232 port. A 2-way 6-port valve (VICI, Cheminert C2-3006D) equipped with a RS-232 port was used to inject an aliquot of the crude mixture within the on-line HPLC unit. The HPLC column outlet was connected to a UV detector (JASCO, UV 2075) equipped with a RS-232

port. The flow outlet was connected to a programmable fraction collector (Advantec, CHF 1225C). All units equipped with a RS-232 port were autonomously controlled with MATLAB[®] through the use of communication protocols provided by the manufacturers.

*Synthesis of (E)-4-methoxy-2-(prop-1-en-1-yl)phenol (6).*¹³ To a solution *n*-BuLi (13.85 mL, 26.3 mmol, 1.9 M in hexane) in distilled THF (65 mL) was added ethyltriphenylphosphonium bromide (9.76 g, 26.3 mmol) at 25 °C. The resulting mixture was stirred for 45 min and then 2-hydroxy-5-methoxybenzaldehyde (2 g, 13.2 mmol) was added in one portion. After being stirred for 3 h, the reaction was quenched with 0.5 M HCl (30 mL) and the aqueous phase was extracted three times with EtOAc (3 × 30 mL). The collected organic extracts were dried over anhydrous MgSO₄, filtered and concentrated under reduced pressure. Purification by flash chromatography (20% EtOAc-petroleum ether) furnished **6** (1.60 g, 74%) as pale yellow liquid. IR (ATR) ν 3372, 3035, 2937, 2912, 2834, 1652, 1607, 1497, 1428, 1280, 1201, 1160, 1037, 968 cm⁻¹. ¹H NMR (300 MHz, CDCl₃) δ 6.86 (d, 1H, *J* = 2.9 Hz), 6.72 (d, 1H, *J* = 8.6 Hz), 6.66 (dd, 1H, *J* = 2.9, 8.7 Hz), 6.57 (dq, 1H, *J* = 1.7, 15.8 Hz), 6.14-6.26 (dq, 1H, *J* = 6.6, 15.8 Hz), 4.73 (br d, 1H, *J* = 2.8 Hz), 3.77 (s, 3H), 1.91 (dd, 3H, *J* = 1.7, 6.6 Hz). ¹³C{¹H} NMR (100 MHz, CDCl₃) δ 153.9, 146.7, 128.4, 126.0, 125.5, 116.6, 113.7, 112.3, 55.9, 19.0. HRMS (ASAP⁺) *m/z* [M + H]⁺ Calcd for C₁₀H₁₃O₂ 165.0916; Found 165.0920

Experimental setup of the automated screening platform. An automatic sample handler prepared 200 μ L of the reaction mixture from stock solutions of 2-propenyl phenol **6** (0.2 M plus xylene as the internal standard at 0.5 M), oxidants (0.4 M) and catalysts (2.5 × 10⁻³ M). The reaction mixture was injected in a stream of C₂H₄Cl₂ pumped at 0.5 mL/min as depicted in Figure 2. The oxidative dimerization occurred either in a PEEK reactor coil (5 mL, 0.75 mm id) heated at the required temperature (25 or 50 °C) for oxidants **8a-c** or in a AF-2400 reactor coil that passed through a glass bottle closed with a GL-45 cap and supplied with a flow of either air or oxygen.²⁹ The reactor outlet was connected to an automatic 2-way 6-port switch valve which injected 0.2 μ L of the crude mixture in the HPLC unit while the remaining stream was collected in a fraction collector. A mixture of MeOH/H₂O (70/30, v/v) was used as mobile phase for the HPLC analysis at a flowrate of 0.4 mL/min. A UV detector was connected to the outlet of the HPLC column (Agela Promosil C18, 3.5 mm × 150 mm, 5 μ m) to follow the absorbance at a wavelength of 270 nm. Peak integration and yield calculation were under full MATLAB automation.

Experimental setup of the autonomous self-optimizing flow reactor. Synthesis of benzoxanthenone (10). An automatic sample handler prepared 200 μ L of the reaction mixture

from stock solutions of 2-propenyl phenol **6** (1 M plus xylene as the internal standard at 2.5 M), *t*-BuOOH **8a** (2 M) and [Co]-**9a** (0.03 M). The reaction mixture was injected in a stream of C₂H₄Cl₂ pumped at the required flow. The oxidative dimerization occurred in a PEEK reactor coil (5 mL, 0.75 mm id) heated at the required temperature. The reactor outlet was connected to an automatic 2-way 6-port switch valve which injected 0.2 μL of the crude mixture in the HPLC unit while the remaining stream was collected in a fraction collector. A mixture of MeOH/H₂O (70/30, v/v) was used as mobile phase for the HPLC analysis at a flowrate of 0.4 mL/min. A UV detector was connected to the outlet of the HPLC column (Agela Promosil C18, 3.5 mm × 150 mm, 5 μm) to follow the absorbance at a wavelength of 270 nm. Peak integration and yield calculation were under full MATLAB automation. The calculated yield was automatically sent to the algorithm which set new experimental conditions to the units via RS-232 ports. A 4-D optimization of the reaction yield was conducted using the temperature, residence time, loading of [Co]-**9a** and equivalents of *t*-BuOOH **8a** as the input variables. The initial experiment of the simplex was: 25 °C, 5 min of residence time, 5 mol% of [Co]-**9a** and 1 equivalent of *t*-BuOOH **8a** with *d* values of 5 °C, 10 min, 2 mol% and 0.2 equivalent, respectively. The lower and upper boundaries of the research space were the following: 25-50 °C, 5-60 min, 1-10 mol% and 1-2 equiv. for the temperature, residence time, catalyst loading and equivalents of oxidant, respectively. An optimum giving 92% HPLC yield was found in experiment 16 at 32 °C, 27 min of residence time, 1 mol% of [Co]-**9a** and 1.09 equivalents of *t*-BuOOH **8a** (see Table S1 for details). An analytical sample of benzoxanthenone **10** was obtained by flash chromatography (10% Et₂O-cyclohexane) as a white solid (23.8 mg, 55%). mp 88.5-89.5 °C. IR (ATR) ν 2958, 2929, 2873, 2835, 1678, 1617, 1492, 1268, 1199, 1115, 1035 cm⁻¹. ¹H NMR (300 MHz, CDCl₃) δ 7.24 (d, 1H, *J* = 10.2 Hz), 7.01-7.03 (m, 1H), 6.89-6.90 (m, 1H), 6.75 (d, 1H, *J* = 8.7 Hz), 6.66 (dd, 1H, *J* = 2.8, 8.8 Hz), 6.31 (d, 1H, *J* = 10.2 Hz), 3.76 (s, 3H), 3.31-3.33 (m, 1H), 3.31 (s, 3H), 3.12-3.16 (m, 1H), 2.59-2.66 (m, 1H), 2.17-2.23 (m, 1H), 1.15 (d, 3H, *J* = 7.2 Hz), 0.67 (d, 3H, *J* = 7.5 Hz). ¹³C{¹H} NMR (75 MHz, CDCl₃) δ 186.8, 154.4, 145.1, 143.7, 142.7, 131.8, 128.1, 125.6, 118.0, 113.6, 113.3, 55.8, 49.3, 37.1, 36.8, 35.2, 34.0, 21.8, 21.4. HRMS (ESI) *m/z* [M + Na]⁺ Calcd for C₂₀H₂₂NaO₄ 349.1416; Found 349.1407.

Synthesis of Carpanone (1). An automatic sample handler prepared 200 μL of the reaction mixture from stock solutions of (*E*)-6-(prop-1-enyl)-1,3-benzodioxol-5-ol **12**¹⁶ (0.25 M, 1 equiv), *t*-BuOOH **8a** (0.5 M, 1.09 equiv) and [Co]-**9a** (0.03 M, 1 mol%). The reaction mixture was injected in a stream of C₂H₄Cl₂ pumped at 0.19 mL/min as depicted in Scheme 1. The oxidative dimerization occurred in a PEEK reactor coil (5 mL, 0.75 mm id) heated at 32 °C.

The reactor outlet was connected to an automatic 2-way 6-port switch valve which injected 0.2 μL of the crude mixture in the HPLC unit while the remaining stream was collected in a fraction collector. A mixture of MeOH/H₂O (70/30, v/v) was used as mobile phase for the HPLC analysis at a flowrate of 0.4 mL/min. A UV detector was connected to the outlet of the HPLC column (Agela Promosil C18, 3.5 mm \times 150 mm, 5 μm) to follow the absorbance at a wavelength of 270 nm. Peak integration and yield calculation were under full MATLAB automation. An analytical sample of carpanone **1** was obtained by flash chromatography (10% Et₂O-cyclohexane) as a white solid (34 mg, 85%). mp 192-193 $^{\circ}\text{C}$ [Lit.¹⁵ 189-190 $^{\circ}\text{C}$]. IR (ATR) ν 2872, 1674, 1622, 1478, 1158, 1032, 910, 840 cm^{-1} . ¹H NMR (400 MHz, CDCl₃) δ 7.00-7.02 (m, 1H), 6.80 (s, 1H), 6.33 (s, 1H), 5.90 (d, 1H, $J = 1.4$ Hz), 5.87 (d, 1H, $J = 1.4$ Hz), 5.69 (s, 1H), 5.66 (s, 1H), 5.64 (s, 1H), 3.27 (dd, 1H, $J = 7.4, 2.6$ Hz), 3.19 (dt, 1H, $J = 7.5, 2.5$ Hz), 2.52 (br qd, 1H, $J = 6.9, 2.1$ Hz), 2.18-2.24 (m, 1H), 1.15 (d, 3H, $J = 7.2$ Hz), 0.71 (d, 3H, $J = 7.6$ Hz). ¹³C{¹H} NMR (100 MHz, CDCl₃) δ 187.0, 168.5, 146.8, 145.3, 143.3, 142.7, 126.5, 115.4, 107.3, 101.4, 100.6, 100.3, 99.4, 98.9, 36.4, 35.6, 35.4, 33.7, 21.6, 21.3. HRMS (ESI) m/z [M + H]⁺ calcd for C₂₀H₁₉O₆, 355.1182, found 355.1180.

5-Allyloxy-1,3-benzodioxole (13). The experimental setup consisted in two streams as depicted in Scheme 2. The first stream contained a solution of sesamol **11** (0.4 M) and KOH (0.6 M) in MeOH/H₂O (95/5, v/v) while the second stream contained a solution of alkyl iodide (0.8 M) in MeOH/H₂O (95/5, v/v). Each solution was continuously pumped with two independent pumps at 32 $\mu\text{L}/\text{min}$ for the first stream and 29 $\mu\text{L}/\text{min}$ for the second stream. The two streams met in a stainless steel T-shaped piece (internal volume: 0.57 μL). The resulting mixture was introduced in a stainless steel reactor coil (2 mL, 0.75 mm id) heated at 75 $^{\circ}\text{C}$. The reactor outlet was connected to a back pressure regulator (BPR) to maintain the internal pressure at *ca.* 15 bar. An analytical sample of 5-allyloxy-1,3-benzodioxole **7** was obtained by flash chromatography (10% AcOEt-petroleum ether) as a colourless oil (1.04 g, 76%). IR (ATR) ν 2283, 1629, 1483, 1178, 1035, 923, 780 cm^{-1} . ¹H NMR (300 MHz, CDCl₃) δ 6.70 (d, 1H, $J = 8.5$ Hz), 6.52 (d, 1H, $J = 2.5$ Hz), 6.34 (dd, 1H, $J = 2.5, 8.5$ Hz), 6.03 (ddt, 1H, $J = 5.3, 10.6, 17.2$ Hz), 5.91 (s, 2H), 5.39 (dq, 1H, $J = 1.6, 17.3$ Hz), 5.28 (dq, 1H, $J = 1.4, 10.5$ Hz), 4.46 (dt, 2H, $J = 1.5, 5.3$ Hz). ¹³C{¹H} NMR (100 MHz, CDCl₃): δ 154.2, 148.3, 141.8, 133.5, 117.7, 108.0, 106.1, 101.2, 98.4, 69.9. HRMS (ASAP+) m/z [M]⁺ Calcd for C₁₀H₁₀O₃ 178.0630; Found 178.0631.

5-Allyloxy-4-formyl-1,3-benzodioxole (14).⁸⁰ A solution of *n*-BuLi (6 mL, 1.6 M) was added dropwise to a solution of 5-allyloxy-1,3-benzodioxole **13** (1.41 g, 7.91 mmol) in dry THF (20 mL) at -78 $^{\circ}\text{C}$. The resulting yellow solution was stirred for 45 min and then dry

DMF (1.25 mL, 15.8 mmol) was added. After 30 min at $-78\text{ }^{\circ}\text{C}$, the reaction mixture was hydrolyzed with saturated NH_4Cl solution and extracted with Et_2O ($3 \times 20\text{ mL}$). The collected organic fractions were dried over anhydrous MgSO_4 , filtered and concentrated under reduced pressure. Purification by flash chromatography (60% CH_2Cl_2 -petroleum ether) furnished the corresponding aldehyde **14** (823 mg, 51%) as a yellow solid. mp $98\text{--}99\text{ }^{\circ}\text{C}$ [Lit.⁸⁰ $98\text{--}100\text{ }^{\circ}\text{C}$]. IR (ATR) ν 2881, 1675, 1630, 1455, 1234, 1075, 913, 745 cm^{-1} . ^1H NMR (300 MHz, CDCl_3) δ 10.42 (s, 1H), 6.89 (d, 1H, $J = 8.6\text{ Hz}$), 6.33 (d, 1H, $J = 8.6\text{ Hz}$), 6.09 (s, 2H), 5.98–6.12 (m, 1H), 5.42 (dq, 1H, $J = 1.6, 17.2\text{ Hz}$), 5.31 (dq, 1H, $J = 1.4, 10.5\text{ Hz}$), 4.56 (dt, 2H, $J = 1.5, 5.2\text{ Hz}$). $^{13}\text{C}\{^1\text{H}\}$ NMR (75 MHz, CDCl_3) δ 188.3, 155.3, 148.5, 142.8, 132.6, 118.1, 113.1, 111.3, 103.8, 103.1, 70.2. HRMS (ESI) m/z $[\text{M} + \text{Na}]^+$ Calcd for $\text{C}_{11}\text{H}_{10}\text{O}_4\text{Na}$ 229.0477; Found : 229.0485.

5-Allyloxy-4-formate-1,3-benzodioxole. *m*-CPBA (5.62 g, 19.5 mmol, 60% in water) was added to a solution of 4-formyl-5-allyloxy-1,3-benzodioxole (2.12 g, 10.3 mmol) in CHCl_3 (34 mL) at $0\text{ }^{\circ}\text{C}$ and the resulting mixture was stirred at $0\text{ }^{\circ}\text{C}$ for 24 h. After completion, the mixture was diluted with chloroform (50 mL) and was successively washed with saturated aqueous Na_2SO_3 solution (50 mL), saturated aqueous Na_2CO_3 solution (50 mL), brine (50 mL) and water (50 mL). The organic phase was dried over anhydrous MgSO_4 and concentrated under reduced pressure. The crude formate was obtained as a yellow oil (1.82 g, 80%) and directly used in the next step without further purification.

5-Allyloxy-4-hydroxy-1,3-benzodioxole (15).⁸⁰ *5-Allyloxy-4-formate-1,3-benzodioxole* (1.82 g, 8.2 mmol) in solution in THF (30 mL) was hydrolyzed by 3N NaOH (9 mL). After being stirred for 1 h at $25\text{ }^{\circ}\text{C}$, the reaction mixture was diluted with CH_2Cl_2 (50 mL). The organic phase was extracted with water ($4 \times 30\text{ mL}$). The aqueous phase was acidified with 2 N HCl and extracted with CH_2Cl_2 ($3 \times 50\text{ mL}$). The organic phases were dried over anhydrous MgSO_4 and concentrated under reduced pressure. Purification by flash chromatography (30% CH_2Cl_2 -petroleum ether) furnished *5-allyloxy-4-hydroxy-1,3-benzodioxole 15* (964 mg, 61%) as a white solid. mp $51\text{--}52\text{ }^{\circ}\text{C}$. IR (ATR) ν 3301, 2902, 1656, 1471, 1244, 1053, 913, 767 cm^{-1} . ^1H NMR (300 MHz, CDCl_3) δ 6.33 (s, 1H), 6.33 (s, 1H), 5.98–6.11 (m, 1H), 5.94 (s, 2H), 5.47 (s, 1H), 5.39 (dq, 1H, $J = 1.5, 17.2\text{ Hz}$), 5.31 (dq, 1H, $J = 1.3, 10.4\text{ Hz}$), 4.53 (dt, 2H, $J = 1.4, 5.5\text{ Hz}$). $^{13}\text{C}\{^1\text{H}\}$ NMR (75 MHz, CDCl_3) δ 143.6, 142.4, 134.1, 133.1, 131.1, 118.6, 104.8, 101.8, 98.9, 71.2. HRMS (ESI) m/z $[\text{M} + \text{Na}]^+$ Calcd for $\text{C}_{10}\text{H}_{10}\text{O}_4\text{Na}$ 217.0477; Found : 217.0470.

5-Allyloxy-4-methoxy-1,3-benzodioxole (16). To a solution of *5-allyloxy-4-hydroxy-1,3-benzodioxole* (1.69 g, 8.70 mmol) in acetone (9 mL) was added sequentially K_2CO_3 (2.40 g,

17.39 mmol) and CH₃I (2.70 ml, 43.48 mmol, 5 equiv). The resulting reaction mixture was stirred at 25 °C for 72 h and then evaporated to dryness under reduced pressure. Inorganic residues were dissolved in water (15 mL) and the aqueous phase was extracted with Et₂O (3 × 15 mL). The collected organic extracts were dried over anhydrous MgSO₄ and concentrated under reduced pressure. Purification by flash chromatography (30% CH₂Cl₂-petroleum ether) furnished 5-Allyloxy-4-methoxy-1,3-benzodioxole **16** as a colorless oil (1.52 g, 84%). IR (ATR) ν 2886, 1630, 1459, 1231, 1049, 923, 778 cm⁻¹. ¹H NMR (300 MHz, CDCl₃) δ 6.42 (d, 1H, *J* = 8.5 Hz), 6.35 (d, 1H, *J* = 8.5 Hz), 5.99-6.12 (m, 1H), 5.90 (s, 2H), 5.37 (dq, 1H, *J* = 1.5, 17.2 Hz), 5.25 (dq, 1H, *J* = 1.3, 10.5 Hz), 4.50 (dt, 2H, *J* = 1.4, 5.4 Hz), 4.00 (s, 3H). ¹³C{¹H} NMR (75 MHz, CDCl₃) δ 146.3, 143.5, 138.2, 135.0, 133.7, 117.7, 107.3, 101.4, 101.3, 71.4, 60.4. HRMS (ESI) *m/z* [M + H]⁺ Calcd for C₁₁H₁₃O₄ 209.0814; Found : 209.0806.

5-hydroxy-4-methoxy-6-(2-propenyl)-1,3-benzodioxole (17). A solution of 5-Allyloxy-4-methoxy-1,3-benzodioxole **16** in acetone (1.5 M) was loaded in a PEEK injection loop (2 mL) connected to a stream of acetone pumped at a flow rate of 2 mL/min as depicted in Scheme 2. The [3,3]-Claisen rearrangement occurred in a stainless steel reactor coil (5 mL, 0.75 mm id) heated at 250 °C. The line was constantly pressurized at 70 bar with an electronic back pressure regulator (BPR) to prevent the vaporization of acetone. The product collected in a flask was concentrated under reduced pressure and the resulting residue was purified by flash chromatography (from 30% CH₂Cl₂-petroleum ether to 50% CH₂Cl₂-petroleum ether) to give **17** as a white solid (791 mg, 89%). mp 31.5-32 °C. IR (ATR) ν 3503, 2885, 1637, 1432, 1176, 1045, 981, 915, 645 cm⁻¹. ¹H NMR (300 MHz, CDCl₃) δ 6.33 (s, 1H), 5.88-6.02 (m, 1H), 5.85 (s, 2H), 5.40 (br s, 1H), 5.02-5.09 (m, 2H), 4.04 (s, 3H), 3.31 (dt, 2H, *J* = 1.2, 6.5 Hz). ¹³C{¹H} NMR (75 MHz, CDCl₃) δ 141.8, 140.0, 136.9, 134.4, 131.2, 117.7, 115.5, 103.0, 101.0, 60.0, 33.9. HRMS (ASAP+) *m/z* [M]⁺ Calcd for C₁₁H₁₂O₄ 208.0736; Found : 208.0736.

(E)-5-hydroxy-4-methoxy-6-(prop-1-enyl)-1,3-benzodioxole (18). A solution of *t*-BuOK in THF (3.5 mL, 3.47 mmol, 1 M, 1.2 equiv) was added to a solution of 5-hydroxy-4-methoxy-6-(2-propenyl)-1,3-benzodioxole **17** (603 mg, 2.90 mmol, 1 equiv) in THF (3 mL) under argon. The resulting mixture was stirred at 70 °C for 90 min and then quenched with water (50 mL) and 5% HCl (10 mL). The aqueous layer was extracted with EtOAc (3 × 30 mL). The collected organic extracts were dried over anhydrous MgSO₄ and concentrated under reduced pressure. Purification by flash chromatography (30% CH₂Cl₂-petroleum ether) furnished **18** as a white solid (295 mg, 49%). mp 66-67 °C. IR (ATR) ν 3382, 2886, 1622,

1422, 1178, 1046, 977, 927, 803 cm^{-1} . ^1H NMR (400 MHz, CDCl_3) δ 6.61 (dq, 1H, $J = 1.5$, 15.8 Hz), 6.58 (s, 1H), 6.08 (dq, 1H, $J = 6.6$, 15.8 Hz), 5.56 (s, 2H), 5.54 (s, 1H), 4.04 (s, 3H), 1.87 (dd, 3H, $J = 1.7$, 6.6 Hz). $^{13}\text{C}\{^1\text{H}\}$ NMR (100 MHz, CDCl_3) δ 142.3, 139.7, 134.9, 131.2, 124.9, 124.8, 116.9, 101.1, 99.0, 60.1, 18.8. HRMS (ESI) m/z $[\text{M} + \text{H}]^+$ Calcd for $\text{C}_{11}\text{H}_{13}\text{O}_4$ 209.0814; Found 209.0806.

Synthesis of Polemannone B (3). An automatic sample handler prepared 200 μL of the reaction mixture from stock solutions of (*E*)-5-methoxy-6-(prop-1-enyl)-1,3-benzodioxol-5-ol **18** (0.25 M, 1 equiv), *t*-BuOOH **8a** (0.5 M, 1.09 equiv) and [Co]-**9a** (0.03 M, 1 mol%). The reaction mixture was injected in a stream of $\text{C}_2\text{H}_4\text{Cl}_2$ pumped at 0.19 mL/min as depicted in Scheme 2. The oxidative dimerization occurred in a PEEK reactor coil (5 mL, 0.75 mm id) heated at 32 $^\circ\text{C}$. The reactor outlet was connected to an automatic 2-way 6-port switch valve which injected 0.2 μL of the crude mixture in the HPLC unit while the remaining stream was collected in a fraction collector. A mixture of MeOH/ H_2O (70/30, v/v) was used as mobile phase for the HPLC analysis at a flowrate of 0.4 mL/min. A UV detector was connected to the outlet of the HPLC column (Agela Promosil C18, 3.5 mm \times 150 mm, 5 μm) to follow the absorbance at a wavelength of 270 nm. Peak integration and yield calculation were under full MATLAB automation. An analytical sample of polemannone B **3** was obtained by flash chromatography (20% Et_2O -cyclohexane) as a white solid (25.2 mg, 84%). mp 160-161 $^\circ\text{C}$ [Lit.⁸¹ 170 $^\circ\text{C}$]. IR (ATR) ν 2899, 1666, 1618, 1429, 1284, 1097, 1044, 888, 758 cm^{-1} . ^1H NMR (400 MHz, CDCl_3) δ 7.03-7.08 (m, 1H), 6.52 (s, 1H), 5.87 (dd, 2H, $J = 1.3$, 14.9 Hz), 5.65 (d, 2H, $J = 8.5$ Hz), 3.96 (s, 3H), 3.93(s, 3H), 3.26 (dd, 1H, $J = 2.6$, 7.6 Hz), 3.17 (dt, 1H, $J = 2.3$, 7.5 Hz) 2.45-2.52 (m, 1H), 2.17-2.26 (m, 1H), 1.13 (d, 3H, $J = 7.1$ Hz), 0.70 (d, 3H, $J = 7.6$ Hz). $^{13}\text{C}\{^1\text{H}\}$ NMR (100 MHz, CDCl_3) δ 183.3, 151.7, 143.9, 143.2, 138.1, 136.0, 133.8, 131.7, 126.6, 117.0, 101.5, 101.3, 100.8, 98.9, 60.4, 59.9, 36.5, 35.8, 35.3, 34.3, 21.6, 21.2. HRMS (ESI) m/z $[\text{M} + \text{Na}]^+$ Calcd for $\text{C}_{22}\text{H}_{22}\text{O}_8\text{Na}$ 437.1212; Found : 437.1205.

■ ASSOCIATED CONTENT

The supporting information is available free of charge on the ACS Publication website at DOI: 10.1021/acs.joc.xxxxxxx

Table S1 and NMR spectra of purified products: **1**, **3**, **6**, **10**, **12**, **13**, **14**, **15**, **16**, **17**, **18** (PDF)

■ AUTHOR INFORMATION

Corresponding author

*E-mail: fx.felpin@univ-nantes.fr

ORCID

François-Xavier Felpin: [0000-0002-8851-246X](https://orcid.org/0000-0002-8851-246X)

Notes

The authors declare no competing financial interest.

■ ACKNOWLEDGEMENTS

This work was supported by the “Région des Pays de la Loire” in the framework of the “Pari Scientifique Régional SmartCat” and the INCa “Institut National du Cancer”. E. C. Aka and M. C. Nongbe thank the "Ministère de l'Enseignement Supérieur et de la Recherche Scientifique de Côte d'Ivoire" for a grant. E.W. gratefully acknowledges the INCa for a grant. D.C.B. gratefully acknowledges the “Région des Pays de la Loire” for a grant. We acknowledge Julie Hémez (CEISAM, University of Nantes) for HRMS analyses.

■ REFERENCES

- (1) Brophy, G. C.; Mohandas, J.; Slaytor, M.; Sternhell, S.; Watson, T. R.; Wilson, L. A. Novel lignans from a cinnamomum sp. from bougainville. *Tetrahedron Lett.* **1969**, *10*, 5159-5162.
- (2) Bae, H.-B.; Li, M.; Son, J.-K.; Seo, C.-S.; Chung, S.-H.; Kim, S.-J.; Jeong, C.-W.; Lee, H.-G.; Kim, W.; Park, H.-C.; Kwak, S.-H. Sauchinone, a lignan from *Saururus chinensis*, reduces tumor necrosis factor- α production through the inhibition of c-raf/MEK1/2/ERK 1/2 pathway activation. *Int. Immunopharmacol.* **2010**, *10*, 1022-1028.
- (3) Gao, Y.; Zhao, H.; Li, Y. Sauchinone prevents IL-1 β -induced inflammatory response in human chondrocytes. *J. Biochem. Mol. Toxicol.* **2018**, *32*, e22033.
- (4) Sung, S. H.; Lee, E. J.; Cho, J. H. E. E.; Kim, H. S.; Kim, Y. C. Sauchinone, a Lignan from *Saururus chinensis*, Attenuates CCl₄-Induced Toxicity in Primary Cultures of Rat Hepatocytes. *Biol. Pharm. Bull.* **2000**, *23*, 666-668.
- (5) Kim, Y. W.; Lee, S. M.; Shin, S. M.; Hwang, S. J.; Brooks, J. S.; Kang, H. E.; Lee, M. G.; Kim, S. C.; Kim, S. G. Efficacy of sauchinone as a novel AMPK-activating lignan for preventing iron-induced oxidative stress and liver injury. *Free Radical Biol. Med.* **2009**, *47*, 1082-1092.

- (6) Kim, Y. W.; Jang, E. J.; Kim, C.-H.; Lee, J.-H. Sauchinone exerts anticancer effects by targeting AMPK signaling in hepatocellular carcinoma cells. *Chem. Biol. Interact.* **2017**, *261*, 108-117.
- (7) Goess, B. C.; Hannoush, R. N.; Chan, L. K.; Kirchhausen, T.; Shair, M. D. Synthesis of a 10,000-Membered Library of Molecules Resembling Carpanone and Discovery of Vesicular Traffic Inhibitors. *J. Am. Chem. Soc.* **2006**, *128*, 5391-5403.
- (8) Lindsley, C. W.; Chan, L. K.; Goess, B. C.; Joseph, R.; Shair, M. D. Solid-Phase Biomimetic Synthesis of Carpanone-like Molecules. *J. Am. Chem. Soc.* **1999**, *122*, 422-423.
- (9) Chapman, O. L.; Engel, M. R.; Springer, J. P.; Clardy, J. C. Total Synthesis of Carpanone. *J. Am. Chem. Soc.* **1971**, *93*, 6696-6698.
- (10) Liron, F.; Fontana, F.; Zirimwabagabo, J.-O.; Prestat, G.; Rajabi, J.; Rosa, C. L.; Poli, G. A New Cross-Coupling-Based Synthesis of Carpanone. *Org. Lett.* **2009**, *11*, 4378-4381.
- (11) Matsumoto, M.; Kuroda, K. Transition Metal(II) Schiff's Base Complexes Catalyzed Oxidation of trans-2-(1-propenyl)-4,5-methylenedioxyphenol to Carpanone by Molecular Oxygen. *Tetrahedron Lett.* **1981**, *22*, 4437-4440.
- (12) Baxendale, I. R.; Lee, A.-L.; Ley, S. V. A Concise Synthesis of Carpanone Using Solid-Supported Reagents and Scavengers. *J. Chem. Soc., Perkin Trans. 1* **2002**, 1850-1857.
- (13) Daniels, R. N.; Fadeyi, O. O.; Lindsley, C. W. A New Catalytic Cu(II)/Sparteine Oxidant System for β,β -Phenolic Couplings of Styrenyl Phenols: Synthesis of Carpanone and Unnatural Analogs. *Org. Lett.* **2008**, *10*, 4097-4100.
- (14) Fadeyi, O. O.; Nathan Daniels, R.; DeGuire, S. M.; Lindsley, C. W. Total Synthesis of Polemannones B and C. *Tetrahedron Lett.* **2009**, *50*, 3084-3087.
- (15) Constantin, M.-A.; Conrad, J.; Meriřor, E.; Koschorreck, K.; Urlacher, V. B.; Beifuss, U. Oxidative Dimerization of (E)- and (Z)-2-Propenylsesamol with O₂ in the Presence and Absence of Laccases and Other Catalysts: Selective Formation of Carpanones and Benzopyrans under Different Reaction Conditions. *J. Org. Chem.* **2012**, *77*, 4528-4543.
- (16) Cortés-Borda, D.; Wimmer, E.; Gouilleux, B.; Barré, E.; Oger, N.; Goulamaly, L.; Peault, L.; Charrier, B.; Truchet, C.; Giraudeau, P.; Rodriguez-Zubiri, M.; Le Grogneq, E.; Felpin, F.-X. An Autonomous Self-Optimizing Flow Reactor for the Synthesis of Natural Product Carpanone. *J. Org. Chem.* **2018**, *83*, 14286-14299.
- (17) Wegner, J.; Ceylan, S.; Kirschning, A. Ten Key Issues in Modern Flow Chemistry. *Chem. Commun.* **2011**, *47*, 4583-4592.
- (18) Ley, S. V. On Being Green: Can Flow Chemistry Help? *Chem. Rec.* **2012**, *12*, 378-390.

- (19) Vaccaro, L.; Lanari, D.; Marrocchi, A.; Strappaveccia, G. Flow Approaches Towards Sustainability. *Green Chem.* **2014**, *16*, 3680-3704.
- (20) Gutmann, B.; Cantillo, D.; Kappe, C. O. Continuous-Flow Technology—A Tool for the Safe Manufacturing of Active Pharmaceutical Ingredients. *Angew. Chem. Int. Ed.* **2015**, *54*, 6688-6728.
- (21) Movsisyan, M.; Delbeke, E. I. P.; Berton, J. K. E. T.; Battilocchio, C.; Ley, S. V.; Stevens, C. V. Taming Hazardous Chemistry by Continuous Flow Technology. *Chem. Soc. Rev.* **2016**, *45*, 4892-4928.
- (22) Plutschack, M. B.; Pieber, B.; Gilmore, K.; Seeberger, P. H. The Hitchhiker's Guide to Flow Chemistry. *Chem. Rev.* **2017**, *117*, 11796-11893.
- (23) Oger, N.; Le Grogneq, E.; Felpin, F.-X. Handling Diazonium Salts in Flow for Organic and Material Chemistry. *Org. Chem. Front.* **2015**, *2*, 590-614.
- (24) Oger, N.; d'Halluin, M.; Le Grogneq, E.; Felpin, F.-X. Using Aryl Diazonium Salts in Palladium-Catalyzed Reactions under Safer Conditions. *Org. Process Res. Dev.* **2014**, *18*, 1786-1801.
- (25) Gavriilidis, A.; Constantinou, A.; Hellgardt, K.; Hii, K. K.; Hutchings, G. J.; Brett, G. L.; Kuhn, S.; Marsden, S. P. Aerobic oxidations in flow: opportunities for the fine chemicals and pharmaceuticals industries. *React. Chem. Eng.* **2016**, *1*, 595-612.
- (26) Hone, C. A.; Kappe, C. O. The Use of Molecular Oxygen for Liquid Phase Aerobic Oxidations in Continuous Flow. *Top. Curr. Chem.* **2018**, *377*, 2.
- (27) Osterberg, P. M.; Niemeier, J. K.; Welch, C. J.; Hawkins, J. M.; Martinelli, J. R.; Johnson, T. E.; Root, T. W.; Stahl, S. S. Experimental Limiting Oxygen Concentrations for Nine Organic Solvents at Temperatures and Pressures Relevant to Aerobic Oxidations in the Pharmaceutical Industry. *Org. Process Res. Dev.* **2015**, *19*, 1537-1543.
- (28) Ye, X.; Johnson, M. D.; Diao, T.; Yates, M. H.; Stahl, S. S. Development of safe and scalable continuous-flow methods for palladium-catalyzed aerobic oxidation reactions. *Green Chem.* **2010**, *12*, 1180-1186.
- (29) O'Brien, M.; Baxendale, I. R.; Ley, S. V. Flow Ozonolysis Using a Semipermeable Teflon AF-2400 Membrane To Effect Gas-Liquid Contact. *Org. Lett.* **2010**, *12*, 1596-1598.
- (30) Brzozowski, M.; O'Brien, M.; Ley, S. V.; Polyzos, A. Flow Chemistry: Intelligent Processing of Gas-Liquid Transformations Using a Tube-in-Tube Reactor. *Acc. Chem. Res.* **2015**, *48*, 349-362.
- (31) Rasheed, M.; Wirth, T. Intelligent Microflow: Development of Self-Optimizing Reaction Systems. *Angew. Chem. Int. Ed.* **2011**, *50*, 357-358.

- (32) Fabry, D. C.; Sugiono, E.; Rueping, M. Self-Optimizing Reactor Systems: Algorithms, On-line Analytics, Setups, and Strategies for Accelerating Continuous Flow Process Optimization. *Isr. J. Chem.* **2014**, *54*, 341-350.
- (33) Fabry, D. C.; Sugiono, E.; Rueping, M. Online Monitoring and Analysis for Autonomous Continuous Flow Self-Optimizing Reactor Systems. *React. Chem. Eng.* **2016**, *1*, 129-133.
- (34) Sans, V.; Cronin, L. Towards Dial-a-Molecule by Integrating Continuous Flow, Analytics and Self-Optimisation. *Chem. Soc. Rev.* **2016**, *45*, 2032-2043.
- (35) Reizman, B. J.; Jensen, K. F. Feedback in Flow for Accelerated Reaction Development. *Acc. Chem. Res.* **2016**, *49*, 1786-1796.
- (36) Henson, A. B.; Gromski, P. S.; Cronin, L. Designing Algorithms To Aid Discovery by Chemical Robots. *ACS Cent. Sci.* **2018**, *4*, 793-804.
- (37) Gromski, P. S.; Henson, A. B.; Granda, J. M.; Cronin, L. How to explore chemical space using algorithms and automation. *Nat. Rev. Chem.* **2019**, *3*, 119-128.
- (38) Krishnadasan, S.; Brown, R. J. C.; deMello, A. J.; deMello, J. C. Intelligent Routes to The Controlled Synthesis of Nanoparticles. *Lab Chip* **2007**, *7*, 1434-1441.
- (39) McMullen, J. P.; Jensen, K. F. An Automated Microfluidic System for Online Optimization in Chemical Synthesis. *Org. Process Res. Dev.* **2010**, *14*, 1169-1176.
- (40) Parrott, A. J.; Bourne, R. A.; Akien, G. R.; Irvine, D. J.; Poliakoff, M. Self-Optimizing Continuous Reactions in Supercritical Carbon Dioxide. *Angew. Chem. Int. Ed.* **2011**, *50*, 3788-3792.
- (41) Moore, J. S.; Jensen, K. F. Automated Multitrajectory Method for Reaction Optimization in a Microfluidic System using Online IR Analysis. *Org. Process Res. Dev.* **2012**, *16*, 1409-1415.
- (42) Skilton, R. A.; Parrott, A. J.; George, M. W.; Poliakoff, M.; Bourne, R. A. Real-Time Feedback Control Using Online Attenuated Total Reflection Fourier Transform Infrared (ATR FT-IR) Spectroscopy for Continuous Flow Optimization and Process Knowledge. *Appl. Spectrosc.* **2013**, *67*, 1127-1131.
- (43) Houben, C.; Peremezhney, N.; Zubov, A.; Kosek, J.; Lapkin, A. A. Closed-Loop Multitarget Optimization for Discovery of New Emulsion Polymerization Recipes. *Org. Process Res. Dev.* **2015**, *19*, 1049-1053.
- (44) Holmes, N.; Akien, G. R.; Savage, R. J. D.; Stanetty, C.; Baxendale, I. R.; Blacker, A. J.; Taylor, B. A.; Woodward, R. L.; Meadows, R. E.; Bourne, R. A. Online Quantitative Mass Spectrometry for the Rapid Adaptive Optimisation of Automated Flow Reactors. *React. Chem. Eng.* **2016**, *1*, 96-100.

- (45) Holmes, N.; Akien, G. R.; Blacker, A. J.; Woodward, R. L.; Meadows, R. E.; Bourne, R. A. Self-Optimisation of the Final Stage in the Synthesis of EGFR Kinase Inhibitor AZD9291 Using an Automated Flow Reactor. *React. Chem. Eng.* **2016**, *1*, 366-371.
- (46) Walker, B. E.; Bannock, J. H.; Nightingale, A. M.; deMello, J. C. Tuning Reaction Products by Constrained Optimisation. *React. Chem. Eng.* **2017**, *2*, 785-798.
- (47) Echtermeyer, A.; Amar, Y.; Zakrzewski, J.; Lapkin, A. Self-Optimisation and Model-Based Design of Experiments for Developing a C–H Activation Flow Process. *Beilstein J. Org. Chem.* **2017**, *13*, 150-163.
- (48) Jeraal, M. I.; Holmes, N.; Akien, G. R.; Bourne, R. A. Enhanced Process Development Using Automated Continuous Reactors by Self-Optimisation Algorithms and Statistical Empirical Modelling. *Tetrahedron* **2018**, *74*, 3158-3164.
- (49) Cherkasov, N.; Bai, Y.; Expósito, A. J.; Rebrov, E. V. OpenFlowChem – a platform for quick, robust and flexible automation and self-optimisation of flow chemistry. *React. Chem. Eng.* **2018**, *3*, 769-780.
- (50) Nelder, J. A.; Mead, R. A Simplex-Method for Function Minimization. *Comput. J.* **1965**, *7*, 308-313.
- (51) McMullen, J. P.; Stone, M. T.; Buchwald, S. L.; Jensen, K. F. An Integrated Microreactor System for Self-Optimization of a Heck Reaction: From Micro- to Mesoscale Flow Systems. *Angew. Chem. Int. Ed.* **2010**, *49*, 7076-7080.
- (52) Bourne, R. A.; Skilton, R. A.; Parrott, A. J.; Irvine, D. J.; Poliakoff, M. Adaptive Process Optimization for Continuous Methylation of Alcohols in Supercritical Carbon Dioxide. *Org. Process Res. Dev.* **2011**, *15*, 932-938.
- (53) Jumbam, D. N.; Skilton, R. A.; Parrott, A. J.; Bourne, R. A.; Poliakoff, M. The Effect of Self-Optimisation Targets on the Methylation of Alcohols Using Dimethyl Carbonate in Supercritical CO₂. *J. Flow Chem.* **2012**, *2*, 24-27.
- (54) Amara, Z.; Streng, E. S.; Skilton, R. A.; Jin, J.; George, M. W.; Poliakoff, M. Automated Serendipity with Self-Optimizing Continuous-Flow Reactors. *Eur. J. Org. Chem.* **2015**, 6141-6145.
- (55) Sans, V.; Porwol, L.; Dragone, V.; Cronin, L. A Self Optimizing Synthetic Organic Reactor System Using Real-Time In-Line NMR Spectroscopy. *Chem. Sci.* **2015**, *6*, 1258-1264.
- (56) Fitzpatrick, D. E.; Battilocchio, C.; Ley, S. V. A Novel Internet-Based Reaction Monitoring, Control and Autonomous Self-Optimization Platform for Chemical Synthesis. *Org. Process Res. Dev.* **2016**, *20*, 386-394.

- (57) Poscharny, K.; Fabry, D. C.; Heddrich, S.; Sugiono, E.; Liauw, M. A.; Rueping, M. Machine Assisted Reaction Optimization: A self-Optimizing Reactor System for Continuous-Flow Photochemical Reactions. *Tetrahedron* **2018**, *74*, 3171-3175.
- (58) Hsieh, H.-W.; Coley, C. W.; Baumgartner, L. M.; Jensen, K. F.; Robinson, R. I. Photoredox Iridium–Nickel Dual-Catalyzed Decarboxylative Arylation Cross-Coupling: From Batch to Continuous Flow via Self-Optimizing Segmented Flow Reactor. *Org. Process Res. Dev.* **2018**, *22*, 542-550.
- (59) Wimmer, E.; Cortés-Borda, D.; Brochard, S.; Barré, E.; Truchet, C.; Felpin, F.-X. An autonomous self-optimizing flow machine for the synthesis of pyridine–oxazoline (PyOX) ligands. *React. Chem. Eng.* **2019**, *4*, 1608-1615.
- (60) Soldatova, N. S.; Postnikov, P. S.; Yusubov, M. S.; Wirth, T. Flow Synthesis of Iodonium Trifluoroacetates through Direct Oxidation of Iodoarenes by Oxone®. *Eur. J. Org. Chem.* **2019**, 2081-2088.
- (61) Baumgartner, L. M.; Coley, C. W.; Reizman, B. J.; Gao, K. W.; Jensen, K. F. Optimum catalyst selection over continuous and discrete process variables with a single droplet microfluidic reaction platform. *React. Chem. Eng.* **2018**, *3*, 301-311.
- (62) Cortés-Borda, D.; Kutonova, K. V.; Jamet, C.; Trusova, M. E.; Zammattio, F.; Truchet, C.; Rodriguez-Zubiri, M.; Felpin, F.-X. Optimizing the Heck–Matsuda Reaction in Flow with a Constraint-Adapted Direct Search Algorithm. *Org. Process Res. Dev.* **2016**, *20*, 1979-1987.
- (63) Shi, G.; Hong, F.; Liang, Q.; Fang, H.; Nelson, S.; Weber, S. G. Capillary-Based, Serial-Loading, Parallel Microreactor for Catalyst Screening. *Anal. Chem.* **2006**, *78*, 1972-1979.
- (64) Goodell, J. R.; McMullen, J. P.; Zaborenko, N.; Maloney, J. R.; Ho, C.-X.; Jensen, K. F.; Porco, J. A.; Beeler, A. B. Development of an Automated Microfluidic Reaction Platform for Multidimensional Screening: Reaction Discovery Employing Bicyclo[3.2.1]octanoid Scaffolds. *J. Org. Chem.* **2009**, *74*, 6169-6180.
- (65) Fang, H.; Xiao, Q.; Wu, F.; Floreancig, P. E.; Weber, S. G. Rapid Catalyst Screening by a Continuous-Flow Microreactor Interfaced with Ultra-High-Pressure Liquid Chromatography. *J. Org. Chem.* **2010**, *75*, 5619-5626.
- (66) Treece, J. L.; Goodell, J. R.; Velde, D. V.; Porco, J. A.; Aubé, J. Reaction Discovery Using Microfluidic-Based Multidimensional Screening of Polycyclic Iminium Ethers. *J. Org. Chem.* **2010**, *75*, 2028-2038.
- (67) Moore, J. S.; Smith, C. D.; Jensen, K. F. Kinetics analysis and automated online screening of aminocarbonylation of aryl halides in flow. *React. Chem. Eng.* **2016**, *1*, 272-279.

- (68) Perera, D.; Tucker, J. W.; Brahmabhatt, S.; Helal, C. J.; Chong, A.; Farrell, W.; Richardson, P.; Sach, N. W. A Platform for Automated Nanomole-Scale Reaction Screening and Micromole-Scale Synthesis in Flow. *Science* **2018**, *359*, 429-434.
- (69) Razzaq, T.; Glasnov, T. N.; Kappe, C. O. Accessing Novel Process Windows in a High-Temperature/Pressure Capillary Flow Reactor. *Chem. Eng. Technol.* **2009**, *32*, 1702-1716.
- (70) Razzaq, T.; Glasnov, T. N.; Kappe, C. O. Continuous-Flow Microreactor Chemistry under High-Temperature/Pressure Conditions. *Eur. J. Org. Chem.* **2009**, 1321-1325.
- (71) Bernhard, G.; Oliver, K. C. Forbidden chemistries — paths to a sustainable future engaging continuous processing. *J. Flow Chem.* **2017**, *7*, 65-71.
- (72) Newton, S.; Carter, C. F.; Pearson, C. M.; Alves, L. D.; Lange, H.; Thansandote, P.; Ley, S. V. Accelerating Spirocyclic Polyketide Synthesis using Flow Chemistry. *Angew. Chem. Int. Ed.* **2014**, *53*, 4915-4920.
- (73) Forster, S.; Rieker, A.; Maruyama, K.; Murata, K.; Nishinaga, A. Cobalt Schiff base complex-catalyzed oxidation of anilines with tert-butyl hydroperoxide. *J. Org. Chem.* **1996**, *61*, 3320-3326.
- (74) Skilton, R. A.; Bourne, R. A.; Amara, Z.; Horvath, R.; Jin, J.; Scully, M. J.; Streng, E.; Tang, S. L. Y.; Summers, P. A.; Wang, J.; Pérez, E.; Asfaw, N.; Aydos, G. L. P.; Dupont, J.; Comak, G.; George, M. W.; Poliakoff, M. Remote-Controlled Experiments with Cloud Chemistry. *Nat. Chem.* **2014**, *7*, 1-5.
- (75) Bédard, A.-C.; Adamo, A.; Aroh, K. C.; Russell, M. G.; Bedermann, A. A.; Torosian, J.; Yue, B.; Jensen, K. F.; Jamison, T. F. Reconfigurable system for automated optimization of diverse chemical reactions. *Science* **2018**, *361*, 1220-1225.
- (76) Ley, S. V.; Ingham, R. J.; O'Brien, M.; Browne, D. L. Camera-Enabled Techniques for Organic Synthesis. *Beilstein J. Org. Chem.* **2013**, *9*, 1051-1072.
- (77) Ley, S. V.; Fitzpatrick, D. E.; Ingham, R. J.; Myers, R. M. Organic Synthesis: March of the Machines. *Angew. Chem. Int. Ed.* **2015**, *54*, 3449-3464.
- (78) Fitzpatrick, D. E.; Ley, S. V. Engineering Chemistry for the Future of Chemical Synthesis. *Tetrahedron* **2018**, *74*, 3087-3100.
- (79) Ley, S. V. The Engineering of Chemical Synthesis: Humans and Machines Working in Harmony. *Angew. Chem. Int. Ed.* **2018**, *57*, 5182-5183.
- (80) Majerus, S. L.; Alibhai, N.; Tripathy, S.; Durst, T. New syntheses of dillapiol [4,5-dimethoxy-6-(2-propenyl)-1,3-benzodioxole], its 4-methylthio and other analogs. *Can. J. Chem.* **2000**, *78*, 1345-1355.

(81) Jakupovic, J.; Eid, F. Benzoxanthenone derivatives from *Polemannia montana*.
Phytochemistry **1987**, 26, 2427-2429.